Applied Physics Letters

Termination-dependence of Fermi level pinning at rare-earth arsenide/GaAs interfaces

Cite as: Appl. Phys. Lett. **116**, 251602 (2020); https://doi.org/10.1063/5.0007479
Submitted: 12 March 2020 . Accepted: 05 June 2020 . Published Online: 22 June 2020

Zhaofu Zhang, Yuzheng Guo, and John Robertson

Appl. Phys. Lett. **116**, 251602 (2020); https://doi.org/10.1063/5.0007479 **116**, 251602

Applied Physics Letters ARTICLE scitation.org/journal/apl

Termination-dependence of Fermi level pinning at rare-earth arsenide/GaAs interfaces

Cite as: Appl. Phys. Lett. **116**, 251602 (2020); doi: 10.1063/5.0007479
Submitted: 12 March 2020 · Accepted: 5 June 2020 ·
Published Online: 22 June 2020

Zhaofu Zhang,[1] Yuzheng Guo,[2] and John Robertson[1,a)]

AFFILIATIONS

[1]Department of Engineering, University of Cambridge, Cambridge CB2 1PZ, United Kingdom
[2]College of Engineering, Swansea University, Swansea SA1 8EN, United Kingdom

[a)]Author to whom correspondence should be addressed: jr@eng.cam.ac.uk

ABSTRACT

The properties of metal/semiconductor interfaces are generally described by the metal-induced gap states (MIGS) model. However, rare-earth (RE) arsenide interfaces are found not to follow the MIGS model in having very different Schottky barrier heights (SBHs) for the Ga- or As-terminations of polar (100) or (111) RE-As/GaAs interfaces. Density function supercell calculations find this effect is due to localized defect interface states located on the mis-coordinated atoms of these interfaces that pin their SBHs at very different energies for each termination as determined by the anion sublattice bonding. Band offsets of semiconducting ScN/GaN interfaces also depend on their termination as determined by the same defect interface states. This pinning mechanism dominates any MIGS mechanism when it arises. Nonpolar (110) interfaces have little change in bonding, so they have no defect interface states, and we find their SBH is pinned by MIGS at the charge neutrality level. Hence, traditional MIGS models should be extended to include such interface states in a more general description.

Pinning of the metal Fermi level (E_F) at an energy in the semiconductor bandgap at metal/semiconductor interfaces limits the controllability of Schottky barrier heights (SBHs) at these interfaces. This limits our ability to reduce the contact resistance of both traditional and low-dimensional semiconductor devices.[1–5] For many semiconductors with moderate bandgap, like Si, Ge, and GaAs or transition metal dichalcogenides (TMDs), the SBH varies quite weakly with metal work function due to a large density of metal-induced gap states (MIGS) at the interface.[6–8] MIGS are the evanescent states of the metal's extended states as they decay into the semiconductor. These states have the same behavior in most metal/semiconductor interfaces and tend to pin E_F near the semiconductor charge neutrality level (CNL).[6–8] For Si or Ge, E_F is pinned in the lower gap[6] or near the valence band maximum (VBM) for Ge.[9]

There are some exceptions to this strong pinning. The clearest exceptions are metal silicides and germanides.[10–14] For silicides on Si, the SBH varies more strongly with their work function than for elemental metals on Si. This de-pinning effect is accompanied by a strong variation of SBH with Si face orientation.[11,12] The E_F shift was found to arise from localized "defect states" near E_F at mis-coordinated sites along the silicide/Si interface.[15,16]

For metals on GaAs and related III–Vs, E_F is pinned at an energy which was first identified as a defect level,[17,18] and then as the CNL.[19,20] A significant exception to strong pinning in the GaAs system is metallic rare-earth (RE) arsenides such as ErAs/GaAs interfaces where the SBH varies with interface orientation from (100), (110) to (111).[21] For a specific orientation, there is an unusually large variation of SBH with the termination, either Ga-first or As-first.[21,22] These exceptions are quite rare so that a special effort should be made to understand its cause in order to find a better model of SBHs and to understand how to control contact resistances more generally. There have been various studies to find the origin of this behavior. To date, Lambrecht *et al.*[23] observed that a type of interface state created different pinning energies for each termination. Delaney *et al.*[24] studied the SBH variations in terms of total valence charge densities and an analysis of the local density of states.

Here, we study Fermi-level de-pinning at RE-As interfaces in a different way. We identify the presence of localized interface defect states as in the silicides, and we link the interface state energies directly to their SBH values for each orientation. Experimentally, most studies of REAs/GaAs interfaces have been for rare-earths with f-states.[25–27] Here, we use the analogous YAs/GaAs interface system. This simplifies the electronic structure calculations by omitting the computational cost of highly correlated 4f levels. We can extrapolate to other RE-arsenides by using their bulk band structures. We also extend the analysis to the related semiconducting ScN/GaN system.

Our calculations use the CASTEP code.[28] The calculations are converged to a residual energy difference of 10^{-5} eV and force tolerance of 0.02 eV/Å. The primitive cell band structures of YAs were calculated by the screened exchange (SX) hybrid functional.[29] SX can also treat f-shells where necessary.[30] For the interface calculations, we used the generalized gradient approximation (GGA) as the electronic exchange-correlation functional and ultra-soft pseudopotentials with a plane wave cut-off energy of 300 eV. The (110) nonpolar interface supercells contain nine layers of RE arsenide and nine layers of GaAs, while the (100) supercells consist of nine layers of RE arsenide and 15 layers of GaAs. A supercell slab with $(\sqrt{2} \times \sqrt{2})$ in-plane periodicity is used to give an even number of electrons and a spinless system. A $5 \times 5 \times 1$ k-point mesh giving 13 k-points was adopted. The supercells contained two interfaces with no vacuum layer. The supercell lattices were relaxed along the z-direction to release any internal stress. Other different relaxation schemes of cell vectors were also compared to test the impact of relaxation on SBH. It turns out that the energy difference is within 40 meV/cell, and they have similar partial density of states (PDOS) curves and SBHs. So the relaxation detail does not have much effect on the defect-induced E_F pinning energies.

Metal arsenides like YAs have two phases: a semiconducting zinc blende (zb) phase and a metallic rock salt (rs) phase (Fig. 1). The rs-YAs is 0.3 eV per formula unit more stable than its zb-phase. The lattice constants of rs-YAs and zb-YAs are 5.83 Å and 5.75 Å, respectively. Our calculated lattice constant of GaAs is 5.78 Å, a 1% mismatch to rs-YAs. The growth of GaAs on rock salt RE-As was studied previously with good lattice-matching.[24–26] Ion channeling shows that the As sublattice is continuous across the interface.[25] STEM lattice images[22] show two interface geometries for the polar (100) orientation, a Ga-terminated interface [Fig. 2(a)], and an As-terminated interface [Fig. 2(b)].

The interface formation energy (E_{form}) depends on the Ga chemical potential μ_{Ga}[24,31] [Fig. 2(f)]. For (100), the Ga-terminated interface is more stable than the As-terminated case, with relatively low formation energy for most of the μ_{Ga} range, shown by solid lines in Fig. 2(f) and experimentally.[23] For the Ga-rich case, E_{form} of Ga-terminated interface is 1.08 eV/cell lower than the As-terminated case.

For the Ga-terminated (100) interface in Fig. 2(a), the Ga sites in the last GaAs layer (labeled as layer 2) remain tetrahedrally coordinated. The As sites in the last YAs layer (layer 1) change from octahedral to sevenfold coordinated. The Y sites in layer 1 change from octahedral to fivefold coordinated. They either gained or lost one bond toward the GaAs side.

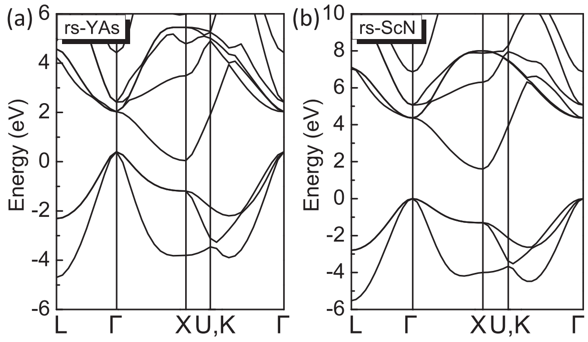

FIG. 1. SX band structures for (a) YAs and (b) ScN bulk, respectively. YAs is a metal, while ScN is a semiconductor with an indirect gap of 1.53 eV, close to the experimental gap of 1.3 ± 0.3 eV.

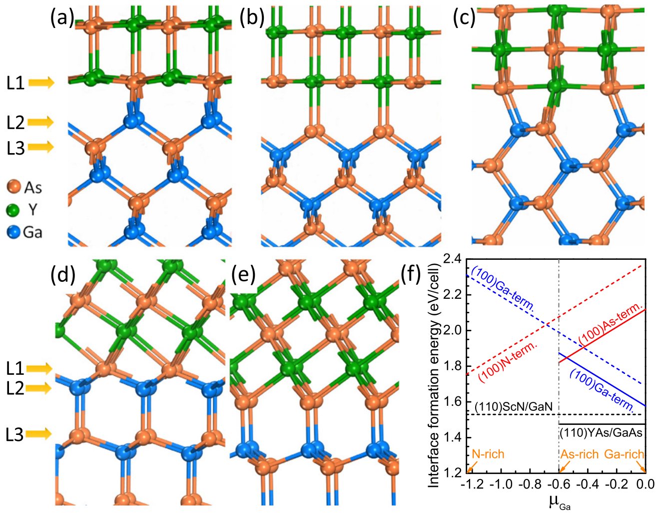

FIG. 2. Atomic structures for YAs/GaAs (a) (100) Ga-termination, (b) (100) As-termination, (c) (110) nonpolar, (d) (111) Ga-termination, and (e) (111) As-termination interfaces, respectively. The interfacial atomic layers are labeled as L1, L2, and L3. (f) shows the interface formation energy, where the solid lines represent YAs/GaAs and dashed lines represent ScN/GaN interfaces, respectively.

The (100) As-termination in Fig. 2(b) has two features. First, the Y sites in layer 1 lie vertically above the interfacial As sites of the GaAs top layer (layer 2). These As sites have now reduced to a threefold coordination, while the Y sites in layer 1 remained sixfold coordinated. However, the As site in layer 1 reduces to being fivefold coordinated. These mis-coordinated atoms are significant for their unusual electronic structures.

Figure 2(c) shows the nonpolar (110) face, where the Ga sites on the GaAs side retain their fourfold bonding, whereas the As sites become fivefold, with two interfacial As-Y bonds per As atom. The Y sites on the YAs side retain their bulk octahedral coordination, while As sites become fivefold coordinated with a dropped bond in the (010) plane. The YAs lattice is displaced relative to the GaAs lattice along the interface, with Y and As sites lying symmetrically above the interfacial Ga–As bond.

The partial density of states (PDOS) for these supercells is calculated. We find a very different behavior compared to the MIGS model of elemental metals and semiconductors. The two (100) interfaces in Fig. 3(a) have a strong orientation dependence, with a p-type SBH of 0.16 eV for As-termination and 1.36 eV for Ga-termination, respectively. The SBHs were obtained using the core-level scheme,[32,33] which takes the energy difference between VBM and core level to stay the same in either isolated bulk or interface material.

The key feature in the electronic structure that causes E_F to vary with termination is the presence of strong localized interfacial gap states around E_F. Previously, Delaney *et al.*[24] considered the band alignments in terms of the electrostatic potential and the total valence charge densities. The gap states in the GaAs in contact with metals would normally be MIGS.[8,20] However, the states around E_F at the YAs/GaAs interface show very unusual behavior. They are localized on the mis-coordinated atoms across the interface. These localized

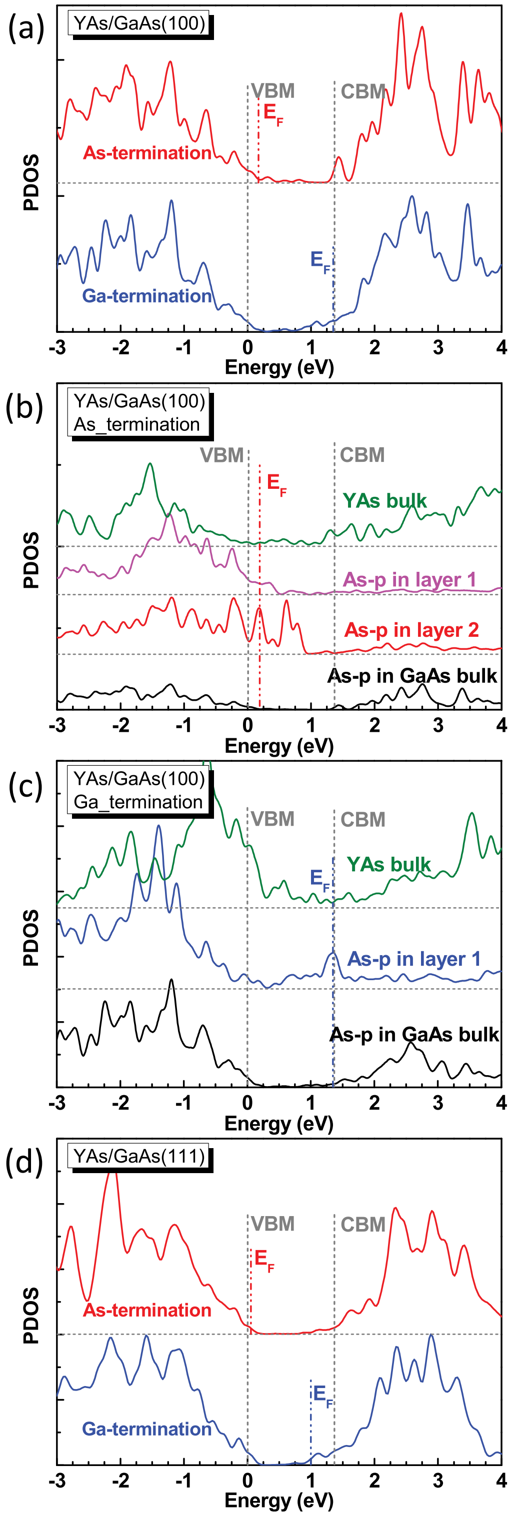

FIG. 3. (a) PDOS of GaAs bulk atoms away from the interface in (100)YAs/GaAs. (b) and (c) are As-p PDOS comparison for two different terminations. (d) PDOS of (111)YAs/GaAs interfaces. VBM is set to 0 eV and E_F is labeled individually.

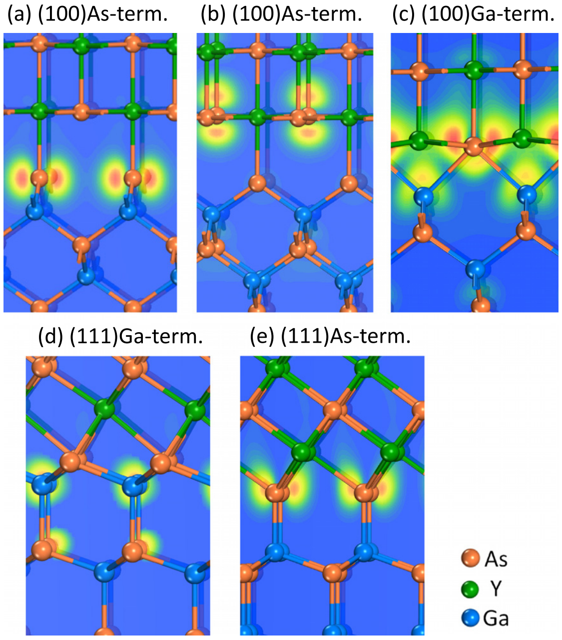

FIG. 4. Wavefunction around E_F for YAs/GaAs. (a) and (b) are two different orbitals around E_F for different viewing angles for (100) As-termination, with localized wavefunction on interfacial threefold (layer 2) and fivefold (layer 1) As atoms, respectively. (c) is (100) Ga-terminated interface. (d) and (e) are (111) Ga- and As-terminations, respectively.

states decay on both the semiconductor side (as in MIGS) and the metal side (unlike MIGS). They are, therefore, "defect-like states" in their localization and similar in character to those seen previously in silicides.[15,16]

The defect states occur at RE-As/GaAs interfaces due to the abrupt change in bonding from the zinc blende GaAs lattice to the rock salt YAs lattice. Although the As sublattice is continuous, the interface creates coordination defects on these sublattices. For the As-terminated interface, the defect states around E_F are localized on the p-π states of threefold As sites in layer 2, as well as the fivefold As in layer 1, as in Figs. 4(a) and 4(b). The interface As-p orbital, with a PDOS peak at E_F [Fig. 3(b)], pins E_F close to the VBM, consistent with the general anion character of the p-orbital. We also built another As-terminated (100)YAs/GaAs, which is a shift of atomic positions of the one in our paper and has fourfold As in layer 2, sevenfold Y, and fivefold As in layer 1 (not shown). Its energy is 180 meV/cell higher than that in Fig. 2(b), but still has similar PDOS and E_F pinning energy.

TABLE I. Calculated p-type SBHs for YAs/GaAs and ScN/GaN interfaces by GGA and SX functional, respectively.

	(100) cation-termination	(100) anion-termination	(110) nonpolar
YAs/GaAs	1.36	0.16	0.50
ScN/GaN[a,b]	1.2	0.05	0.51

[a] VBO for ScN/GaN.

[b] SX functional for ScN/GaN.

On the other hand, the defect state of the Ga-terminated (100) interface is localized on the sevenfold As sites in layer 1 and fourfold Ga sites in layer 2, and this pins E_F near the CBM, Fig. 4(c). The wavefunction around E_F is not on the fivefold Y site with its "dangling bond," as mentioned in Ref. 23. The cationic Ga-s states would normally have an energy close to CBM, while the anionic As-p states are close to the VBM. However, the PDOS calculation finds that the sevenfold As-sites in layer 1 have pushed these As states up in the GaAs gap to lie near the CBM. Hence, the pinning energy is near the CBM by defect states on As-sites as well as on Ga-sites, as seen in the PDOS, Fig. 3(c).

For the Ga-terminated (111) interface, the As sites in layer 1 are sixfold coordinated, the same as in bulk YAs, but unlike the fourfold As in bulk GaAs [Fig. 2(d)]. We find interfacial defect gap states localized on Ga-sites in layer 2 and As sites in layer 3, Fig. 4(d). The defect states on As-sites are like for the (100) Ga-termination case, forced up toward the CBM. Together with defect states on Ga-sites, they pin E_F at 1.0 eV above VBM, Fig. 3(d).

For the As-terminated (111) interface, the last As sites of the YAs lie directly above the last Ga sites of the GaAs. Here, there is a defect gap state localized on the As states, [Fig. 4(e)], and this pins E_F at 0.05 eV above the VBM, Fig. 3(d). Thus, the Fermi energies for each of these polar interfaces are explained by the energies of the associated interface defect gap states, not the CNLs. Thus, the defect states have a sufficient density to pin E_F at very different energies for the two terminations, much further apart than the 0.3 eV separation that a dipole layer causes in other GaAs Schottky barriers.[34]

For the nonpolar (110)YAs/GaAs interfaces, there are no defect gap states and E_F is pinned near midgap at 0.50 eV by MIGS. There are no defect interface states because the interface involves no mis-coordinated sites as shown in Fig. 2(c). Thus, the (110) behaves like a Schottky barrier pinned by normal MIGS with a single pinning energy very close to the CNL energy of 0.54 eV (Table I). But for (100) and (111) interfaces, their mis-coordinated sites induce localized defect interface states, with a high local DOS. Their DOS dominate any underlying MIGS and give very different pinning energies for the two different terminations.

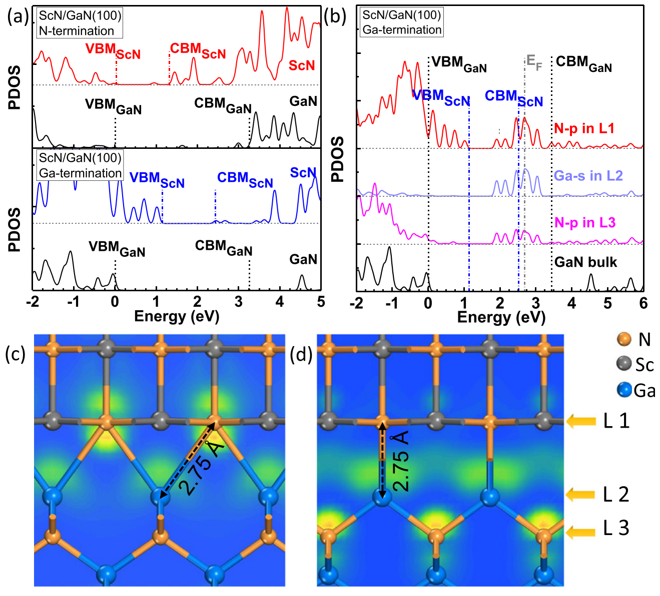

FIG. 5. (a) SX PDOS of GaN and ScN bulk atoms away from the interface in (100)ScN/GaN. (b) PDOS comparison between the GaN bulk and the interfacial atoms in Ga-terminated interface. The VBM of GaN bulk is aligned to 0 eV. (c) and (d) are two different orbitals around E_F (∼2.7 eV above GaN's VBM) and the PDOS peak at 1.9 eV above VBM for Ga-terminated interface, respectively.

We now consider the ScN/GaN interface. Although rock salt ScN is a semiconductor with a 1.3 eV gap[35,36] rather than a metal as YAs (Fig. 1), the ScN/GaN interfaces also possess interface "defect gap states" which turn out to give band offsets which vary with termination. The ScN/GaN interface is a type I band alignment. GGA functional gives a metal behavior for ScN, so the calculated PDOSs use the SX functional, which is also confirmed by HSE functional, as in Fig. 5. The distinct orientation-dependent E_F pinning energies are shown in Fig. 5(a). A 1.2 eV shift is a huge variation in VBO with termination.

The defect gap state for N-terminated interface lies on the interfacial N-sites and the VBM of ScN is pinned near VBM of GaN, as in the As-terminated GaAs interface in Fig. 4(a). This gives a VBO of ∼0 eV. In contrast, the SX PDOS of the Ga-terminated ScN/GaN interface is more complicated, with one peak around E_F (∼2.7 eV above GaN's VBM) and another peak at ∼1.9 eV [Fig. 5(b)]. This is caused by the relatively longer interfacial Ga–N bond [2.75 Å shown in Figs. 5(c) and 5(d)], much longer than the bulk Ga–N bond length of 2.0 Å. This causes its higher interface formation energy than the YAs/GaAs interface [dashed lines in Fig. 2(f)]. Hence, both the N-p orbitals in layer 1 and the Ga-s in layer 2 give a defect gap state lying near the E_F as shown in Fig. 5(c). Hence, the band-edges of ScN are forced upward, giving a VBO of ∼1.2 eV, Fig. 5(a). The other peak lying 1.9 eV above VBM is caused by the interfacial Ga-s and N-p orbitals as shown by the wavefunction in Fig. 5(d). Thus, the band offsets in the YAs/GaAs and ScN/GaN systems are both controlled by the anionic sublattice as they control the anion (As/N) terminated interfaces directly, and for the cation (Ga)-terminated case, they set the SBH/VBO shift by the anion bonding.

The ScN/GaN interface is of particular interest because of its large change in band offset with different terminations. This is controlled by nitrogen sites for both terminations, and it is interesting that N bonding can cause a pinning energy shift (i.e., VBO) of 1.2 eV from Ga- to N-termination, following the same mechanism as in the YAs/GaAs case.

Thus, the ScN/GaN semiconductor interface behaves differently to typical semiconductor heterojunctions. Usually, their band offsets vary little with face orientation, and the main discussion is whether the band offset mainly follows an alignment with an absolute reference energy such as the vacuum level or a core level,[37,38] or with the internal alignment of each semiconductor's CNLs.[38,39] When there is a dependence on face termination (under anion-rich or cation-rich ambient), it gives rise to a dipole layer, and this usually causes a significant band offset variation which follows the valence charge distribution.[40] However, here the SBH or VBO shift arises mostly from different pinning energies due to the different defect gap states for each termination. It is unusual to be as large as 1.2 eV in ScN/GaN. However, a disadvantage of this mechanism is that it adds gap states within the smaller gap of the type I alignment at the semiconductor interface, which is a disadvantage for electronic devices compared to normal alignment schemes.[20,40] The interface defect position and density could be experimentally measured by electrical or spectroscopy characterizations, but a quantitative comparison between the calculated results and experimental measurements is still difficult at the moment.

In conclusion, the MIGS model is generally applicable to many semiconductor/metal systems, but not all. We have identified the rare-earth arsenide/GaAs interface as one specific case where the standard MIGS model does not hold. It is found that the (100) interfaces with different terminations show obviously different Schottky barrier heights and, thus, different pinning energies. This is due to the mis-coordinated atoms at the interface. The states localize at the interface, and decay into both the semiconductor side and metal side. These observations are useful to help identify other systems with mis-coordinated interface sites so that we can tune the Fermi level, modify the Schottky barrier heights, and, thus, design devices with lower contact resistances, which are needed for both highly scaled Si devices and modern 2D semiconductor systems.

The authors acknowledge funding from EPSRC Grant No. EP/P005152/1. We also thank Supercomputing Wales for support under Project No. SCW1070.

DATA AVAILABILITY

The data that support the findings of this study are available from the corresponding author upon reasonable request.

REFERENCES

[1] A. Allain, J. Kang, K. Banerjee, and A. Kis, Nat. Mater. **14**, 1195 (2015).
[2] S. Lee, A. Tang, S. Aloni, and H. S. Philip Wong, Nano Lett. **16**, 276 (2016).
[3] C. Kim, I. Moon, D. Lee, M. Choi, F. Ahmed, S. Nam, Y. Cho, H. Shin, S. Park, and W. Yoo, ACS Nano **11**, 1588 (2017).
[4] G. Kim, S. Kim, J. Park, K. H. Han, J. Kim, and H. Yu, ACS Nano **12**, 6292 (2018).
[5] Y. Liu, J. Guo, E. Zhu, L. Liao, S. Lee, M. Ding, I. Shakir, V. Gambin, Y. Huang, and X. Duan, Nature **557**, 696 (2018).
[6] J. Tersoff, Phys. Rev. Lett. **52**, 465 (1984); Phys. Rev. B **32**, 6968(R) (1985).
[7] W. Monch, Phys. Rev. Lett. **58**, 1260 (1987).
[8] J. Robertson, J. Vac. Sci. Technol., B **18**, 1785 (2000).
[9] A. Dimoulas, P. Tsipas, A. Sotiropoulos, and E. K. Evangelou, Appl. Phys. Lett. **89**, 252110 (2006).
[10] L. Lin, Y. Guo, and J. Robertson, Appl. Phys. Lett. **101**, 052110 (2012).
[11] H. Li, Y. Guo, and J. Robertson, Sci. Rep. **7**, 16669 (2017).
[12] J. L. Freeouf, Solid State Commun. **33**, 1059 (1980).
[13] R. T. Tung, Phys. Rev. Lett. **52**, 461 (1984).
[14] T. Nishimura, T. Yajima, and A. Toriumi, Appl. Phys. Express **9**, 081201 (2016).
[15] Z. Zhang, Y. Guo, and J. Robertson, "Apparent Fermi level depinning and localized interface states at metal silicide Schottky barriers" (unpublished) (2020).
[16] H. Fujitani and S. Asano, Phys. Rev. B **50**, 8681 (1994).
[17] W. E. Spicer, I. Lindau, P. Skeath, C. Y. Su, and P. Chye, Phys. Rev. Lett. **44**, 420 (1980).
[18] R. E. Allen, T. J. Humphreys, J. D. Dow, and O. F. Sankey, J. Vac. Sci. Tecnol., B **2**, 449 (1984).
[19] F. Flores and C. Tejedor, J. Phys. C **20**, 145 (1987).
[20] J. Robertson, Appl. Phys. Lett. **94**, 152104 (2009).
[21] C. J. Palmstrøm, T. L. Cheeks, H. L. Gilchrist, J. G. Zhu, C. B. Carter, B. J. Wilkens, and R. Martin, J. Vac. Sci. Technol., A **10**, 1946 (1992).
[22] D. O. Klenov, J. M. Zide, J. D. Zimmerman, A. C. Gossard, and S. Stemmer, Appl. Phys. Lett. **86**, 241901 (2005).
[23] W. R. L. Lambrecht, A. G. Petukhov, and B. T. Hemmelman, Solid State Commun. **108**, 361 (1998).
[24] K. T. Delaney, N. A. Spaldin, and C. G. Van de Walle, Phys. Rev. B **81**, 165312 (2010).
[25] A. Guivarc'h, Y. Ballini, M. Minier, B. Guenais, G. Dupas, G. Ropars, and A. Regreny, J. Appl. Phys. **73**, 8221 (1993).
[26] J. D. Zimmerman, E. R. Brown, and A. C. Gossard, J. Vac. Sci. Technol., B **23**, 1929 (2005); M. P. Hanson, S. R. Bank, J. M. O. Zide, J. D. Zimmerman, and A. C. Gossard, J. Cryst. Growth **301**, 4 (2007).
[27] S. Khalid, A. Sharan, and A. Janotti, Phys. Rev. B **101**, 125105 (2020).
[28] S. J. Clark, M. D. Segall, C. J. Pickard, P. J. Hasnip, M. J. Probert, K. Refson, and M. C. Payne, Z. Kristallogr. **220**, 567 (2005).
[29] S. J. Clark and J. Robertson, Phys. Rev. B **82**, 085208 (2010).
[30] R. Gillen, S. J. Clark, and J. Robertson, Phys. Rev. B **87**, 125116 (2013).
[31] Z. Zhang, R. Cao, C. Wang, H. Li, H. Dong, W. Wang, F. Lu, Y. Cheng, X. Xie, H. Liu, K. Cho, R. Wallace, and W. Wang, ACS Appl. Mater. Interfaces **7**, 5141 (2015).
[32] E. A. Kraut, R. W. Grant, J. R. Waldrop, and S. P. Kowalczyk, Phys. Rev. Lett. **44**, 1620 (1980).
[33] Z. Zhang, Y. Guo, and J. Robertson, Appl. Phys. Lett. **114**, 161601 (2019).
[34] C. Berthod, N. Binggeli, and A. Baldereschi, Phys. Rev. B **68**, 085323 (2003).
[35] D. Gall, M. Städele, K. Järrendahl, I. Petrov, P. Desjardins, R. T. Haasch, T. Y. Lee, and J. E. Greene, Phys. Rev. B **63**, 125119 (2001).
[36] C. Stampfl, W. Mannstadt, R. Asahi, and A. J. Freeman, Phys. Rev. B **63**, 155106 (2001).
[37] S. H. Wei and A. Zunger, Appl. Phys. Lett. **63**, 2549 (1993).
[38] Y. Hinuma, A. Gruneis, G. Kresse, and F. Oba, Phys. Rev. B **90**, 155405 (2014).
[39] Y. Guo, H. Li, S. J. Clark, and J. Robertson, J. Phys. Chem. C **123**, 5562 (2019).
[40] J. Tersoff, Phys. Rev. B **30**, 4874 (1984).